Original Article

Radiation dose of cone beam CT combined with shape sensing robotic assisted bronchoscopy for the evaluation of pulmonary lesions: an observational single center study

Kim Styrvoky[1]^, Audra Schwalk[1], David Pham[1], Kristine Madsen[2], Hsienchang T. Chiu[1], Muhanned Abu-Hijleh[1]

[1]Division of Pulmonary and Critical Care Medicine, University of Texas Southwestern Medical Center, Dallas, TX, USA; [2]Department of Internal Medicine, University of Texas Southwestern Medical Center, Dallas, TX, USA

Contributions: (I) Conception and design: K Styrvoky, M Abu-Hijleh; (II) Administrative support: None; (III) Provision of study materials or patients: K Styrvoky, A Schwalk, HT Chiu, M Abu-Hijleh; (IV) Collection and assembly of data: K Styrvoky, D Pham, K Madsen; (V) Data analysis and interpretation: K Styrvoky, A Schwalk, M Abu-Hijleh; (VI) Manuscript writing: All authors; (VII) Final approval of manuscript: All authors.

Correspondence to: Kim Styrvoky, MD. Division of Pulmonary and Critical Care Medicine, University of Texas Southwestern Medical Center, 5323 Harry Hines Blvd, Dallas, TX 75219, USA. Email: kim.styrvoky@utsouthwestern.edu.

Background: Shape sensing robotic-assisted bronchoscopy (ssRAB) combined with radial endobronchial ultrasound (r-EBUS) and cone beam computed tomography (CBCT) is a newer diagnostic modality for the evaluation of pulmonary lesions. There is limited data describing the radiation dose of CBCT combined with ssRAB. The purpose of this study was to describe the technical factors associated with the use of CBCT combined with ssRAB to biopsy pulmonary lesions.

Methods: We conducted a single center, prospective observational study of patients undergoing ssRAB combined with fixed CBCT for the pulmonary lesion biopsy. We report our patient demographics, and pulmonary lesion and procedure characteristics.

Results: A total of 241 ssRAB procedures were performed to biopsy 269 pulmonary lesions. The mean lesion size was measured in the following dimensions: anteroposterior (18.0±8.8 mm), transverse (17.2±10.5 mm), and craniocaudal (17.7±10.2 mm). A mean of 1.5±0.7 (median: 1, range: 1–4) CBCT spins were performed. The mean total fluoroscopy time (FT) was 5.6±2.9 minutes. The mean radiation dose of cumulative air kerma (CAK) was 63.5±46.7 mGy and the mean cumulative dose area product (DAP) was 22.6±16.0 Gy·cm^2. Diagnostic yield calculated based on results at index bronchoscopy was 85.9%. There was a low rate of complications with 8 pneumothoraces (3.3%), 5 (2.1%) of which required chest tube placement.

Conclusions: We describe the use of ssRAB combined with CBCT to biopsy pulmonary lesions as a safe diagnostic modality with relatively low radiation dose that is potentially comparable to other image guided sampling modalities. Bronchoscopists should be cognizant of the radiation use during the procedure for both patient and staff safety.

Keywords: Robotic assisted bronchoscopy (RAB); navigational bronchoscopy; cone beam computed tomography (CBCT); radiation dose; pulmonary lesion

Submitted Apr 08, 2023. Accepted for publication Aug 18, 2023. Published online Aug 30, 2023.
doi: 10.21037/jtd-23-587
View this article at: https://dx.doi.org/10.21037/jtd-23-587

^ ORCID: 0000-0002-9186-9187.

Introduction

Bronchoscopic diagnostic modalities for the evaluation of pulmonary lesions have progressed over the years from traditional bronchoscopy to pre-planning software allowing for virtual navigational bronchoscopy combined with ultra-thin bronchoscopy, followed by manual electromagnetic navigational bronchoscopy (ENB), and more recently, robotic assisted bronchoscopy (RAB) using electromagnetic or shape sensing technology. The evolution of diagnostic bronchoscopy has been additive, with each advancement building on existing tools and technologies. The development of RAB allows for navigation to central and peripheral target lesions under direct vision with easy catheter maneuverability, precise catheter tip articulation and stability using a robotic arm. The Ion endoluminal system by Intuitive Surgical, Inc. (Sunnyvale, CA, USA) utilizes shape sensing technology for navigation.

Recent single center studies using shape sensing robotic-assisted bronchoscopy (ssRAB) have shown favorable diagnostic outcomes (1-5). A challenge to improve diagnostic accuracy in the evaluation of pulmonary lesions has been to overcome computed tomography (CT)-to-body divergence. CT-to-body divergence is the difference between the nodule location in a pre-procedure CT scan, when the patient performs a full negative inspiratory breath, and the actual location of the nodule intraprocedurally while the patient is under general anesthesia with positive pressure ventilation at tidal volumes (6). Other procedure specific factors that lead to CT-to-body divergence include nodule motion, relationship of the nodule to the adjacent airways, and the development of atelectasis during the procedure (6,7). Ventilator protocols have been developed to reduce atelectasis and minimize motion during navigational bronchoscopy procedures (8,9).

As a result of technical challenges due to CT-to-body divergence and to allow for real-time confirmation of lesion location, adjunct imaging modalities are often utilized after navigation and during sampling. These adjunct imaging modalities include radial endobronchial ultrasound (r-EBUS), digital tomosynthesis, cone beam computed tomography (CBCT), and augmented fluoroscopy (10).

CBCT is a CT modality that is compact enough to allow mounting on a moving C-arm and is used by multiple medical specialties during diagnostic and interventional procedures (11-13). CBCT can be fixed or mobile. Mobile CBCT allows for portability between procedural or surgical rooms. Volumetric data acquisition is performed in a single rotation of the source and detector while the patient remains stationary. Images are reconstructed to allow viewing in coronal, sagittal, and axial planes. Software packages can then allow for nodule segmentation for viewing in 3-dimensional (3D) reconstructions and for 2-dimensional (2D) fluoroscopy overlays during augmented fluoroscopy (10,14). Fixed CBCT has a short image acquisition time (5–10 seconds) with high quality imaging while mobile CBCT has a longer image acquisition time (30 seconds) with potentially lower imaging quality; cost and lack of portability are barriers to fixed CBCT as compared to mobile CBCT (10,15).

CBCT usage has been described with guided bronchoscopy techniques such as ultrathin/thin bronchoscopy (16,17), manual ENB (18-20) and ssRAB (2,4,15). However, there has been minimal published data regarding CBCT procedural specifics and radiation dose when combined with ssRAB. We performed a single center, observational prospective study to detail patient, nodule, and procedural specifics using ssRAB combined with a fixed CBCT for the evaluation of pulmonary lesions. We present this article in accordance with the STROBE reporting checklist (available at https://jtd.amegroups.com/article/view/10.21037/jtd-23-587/rc).

Highlight box

Key findings

- Robotic assisted bronchoscopy (RAB) with cone beam computed tomography (CBCT) guidance to biopsy pulmonary lesions is a safe diagnostic modality with relatively low radiation dose potentially comparable to other image-guided sampling modalities.

What is known and what is new?

- CBCT is an advanced imaging modality used in diagnostic and interventional procedures.
- We performed a single center, observational study to describe the radiation dose associated with CBCT combined with RAB to biopsy pulmonary lesions.

What is the implication, and what should change now?

- With the addition of advanced imaging modalities, bronchoscopists should be cognizant of the radiation dose during the procedure for both patient and staff safety.

Methods

This was a prospective observational study of all consecutive patients who underwent ssRAB procedures using the Ion endoluminal system to sample pulmonary lesions between

February 25, 2022 and March 8, 2023 at the University of Texas Southwestern Medical Center (UTSW). Five interventional pulmonologists performed the ssRAB procedures. The study was conducted in accordance with the Declaration of Helsinki (as revised in 2013). The study was approved by UT Southwestern Institutional Review Board (No. STU-2021-0346) and individual consent for this analysis was waived. Patients were included for analysis if the procedure utilized CBCT with available radiological data. Prospective data collection is ongoing.

Procedure

Our robotic bronchoscopy procedural technique has previously been described (4) and CBCT was performed using a ceiling-mounted system (Philips Allura FD20 platform with the XperGuide software; Best, The Netherlands). All procedures received onsite intraprocedural support from a dedicated registered radiologic technologist [RT(R)]. The RT(R) used clinical judgment to select pre-set system parameters for the CBCT (8 second spin at normal, 50%, or 25% dose) and fluoroscopy (low, medium, or normal) depending on the patient's body habitus and body mass index which can affect image quality and clarity. The technician then performed the CBCT spin (either at tidal volumes, end inspiratory breath hold, or forced vital capacity maneuver, at the discretion of the bronchoscopist). The bronchoscopist reviewed the images and performed nodule segmentation (*Figures 1,2*). The RT(R) also assisted during the procedure by arranging augmented fluoroscopy for viewing the segmented nodule with 2D fluoroscopy, adjusting the C-arm for different fluoroscopic angles, and digitally zooming fluoroscopic images during sampling. The settings were at the discretion of RT(R). During r-EBUS use, catheter adjustments, or sampling, fluoroscopy was utilized in either a continuous or pulsed manner. All precautions were taken to minimize radiation exposure to patients and staff per standard radiation safety protocols. As an example, all staff are asked to leave the room during a CBCT spin to reduce radiation exposure with close visual and digital monitoring of the patient.

Outcomes

Clinical data collected from medical records included patient demographics, lesion characteristics, and procedural specifics. The lesion location (central, middle, or peripheral) was determined using the concentric line pattern (21). R-EBUS was documented as concentric, eccentric, or could not be visualized as per the procedure report; the most optimal view obtained during the procedure was recorded.

We recorded the use of advanced imaging during the procedure, including the number of CBCT spins performed, if the bronchoscopist subjectively reported significant CT-to-body divergence affecting the procedure in their procedure report, fluoroscopy time (FT; in minutes), radiation dose in cumulative air kerma (CAK; mGy), and cumulative dose area product (DAP; Gy·cm^2). We did not require confirmation of tool in lesion on CBCT imaging.

Study data were collected and managed using REDCap (Research Electronic Data Capture) electronic data capture tools hosted at UT Southwestern Medical Center and supported by CTSA Grant Number UL1 TR003163 from the National Center for Advancing Translational Science (NCATS), a component of the National Institutes of Health (NIH). The content is solely the responsibility of the authors and does not necessarily represent the official views of the NIH. REDCap is a secure, web-based software platform designed to support data capture for research studies, providing (I) an intuitive interface for validated data capture; (II) audit trails for tracking data manipulation and export procedures; (III) automated export procedures for seamless data downloads to common statistical packages; and (IV) procedures for data integration and interoperability with external sources (22,23).

Statistical analysis

We used descriptive statistics for the patient demographics, nodules, and procedural characteristics. We report statistics as counts and percentages, means with standard deviations, and medians with ranges, where appropriate. Diagnostic yield was calculated based on pathology and cytology results at index bronchoscopy with no additional follow-up information using method 2 as described by Vachani *et al.* (24). Independent samples *t*-test was performed to compare means. Binary logistic regression analysis was performed to evaluate associations between procedure factors and diagnostic yield. Statistical tests were two-tailed, and a P value of <0.05 was considered statistically significant. Analysis was performed using Microsoft Excel 2016 (Microsoft Corporation, Redmond, WA, USA) and IBM SPSS Statistics for Windows, Version 28.0 (IBM Corporation, Armonk, NY, USA).

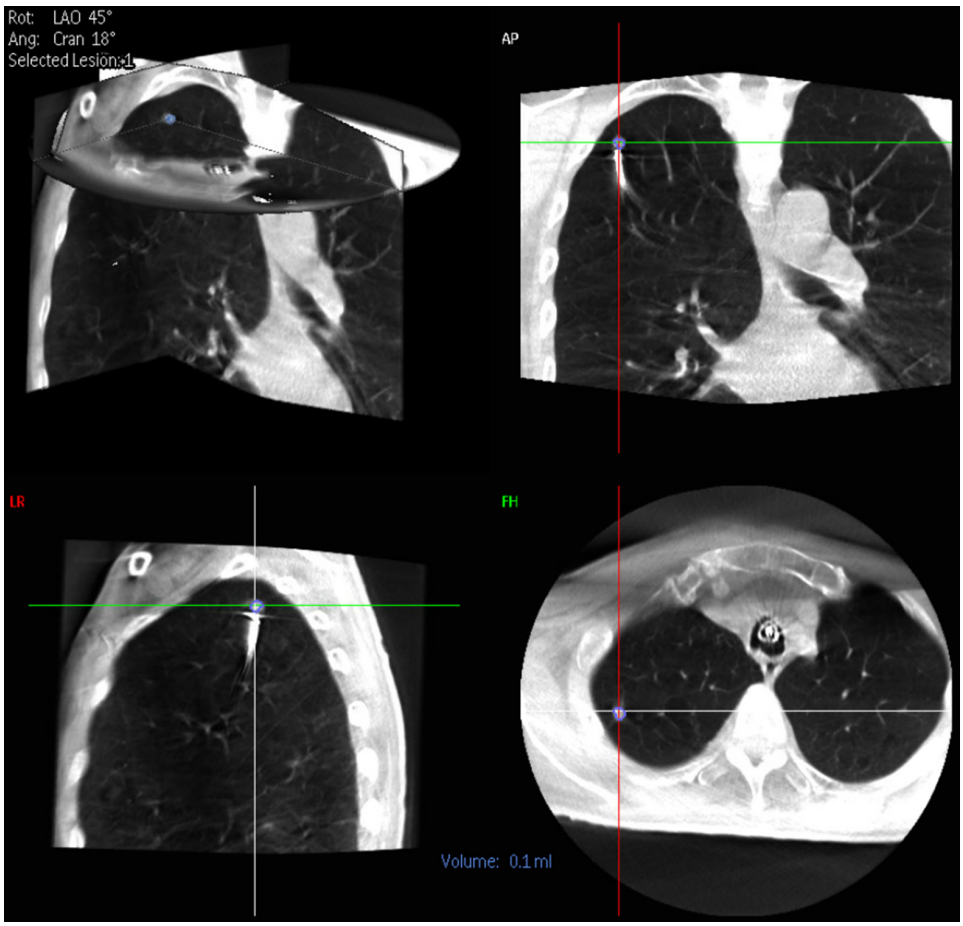

Figure 1 Nodule segmentation view with 9 mm right upper lobe nodule selected in coronal, sagittal and axial views. LAO, left anterior oblique; AP, anterior to posterior; LR, left to right; FH, foot to head.

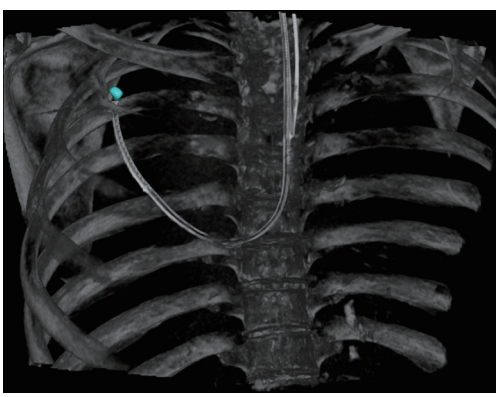

Figure 2 Three-dimensional reconstruction of segmented nodule in relation to ssRAB catheter as viewed in LAO 45°. Image able to be rotated real-time to visualize catheter-to-lesion positioning. ssRAB, shape sensing robotic-assisted bronchoscopy; LAO, left anterior oblique.

Results

Patient and nodule characteristics

During the study period, 282 ssRAB procedures to biopsy 315 lung nodules were performed at our institution. Shape sensing RAB with CBCT was used in 245 procedures to biopsy 275 lung nodules. In our study, we included 241 ssRAB with CBCT procedures to biopsy 269 lung nodules that had available radiological data in the analysis. *Figure 3* details a flow chart for patient selection for inclusion.

The mean age was 67.8±10.7 years with a 56% female predominance. 63.9% were either active or former smoking tobacco users. In terms of nodule characteristics, the mean lesion size was measured in three dimensions: anteroposterior (18.0±8.8 mm), transverse (17.2±10.5 mm), and craniocaudal (17.7±10.2 mm) with a median size for largest dimension of 18.40 mm (interquartile range, 13.3–25.6 mm). Only 7.1%

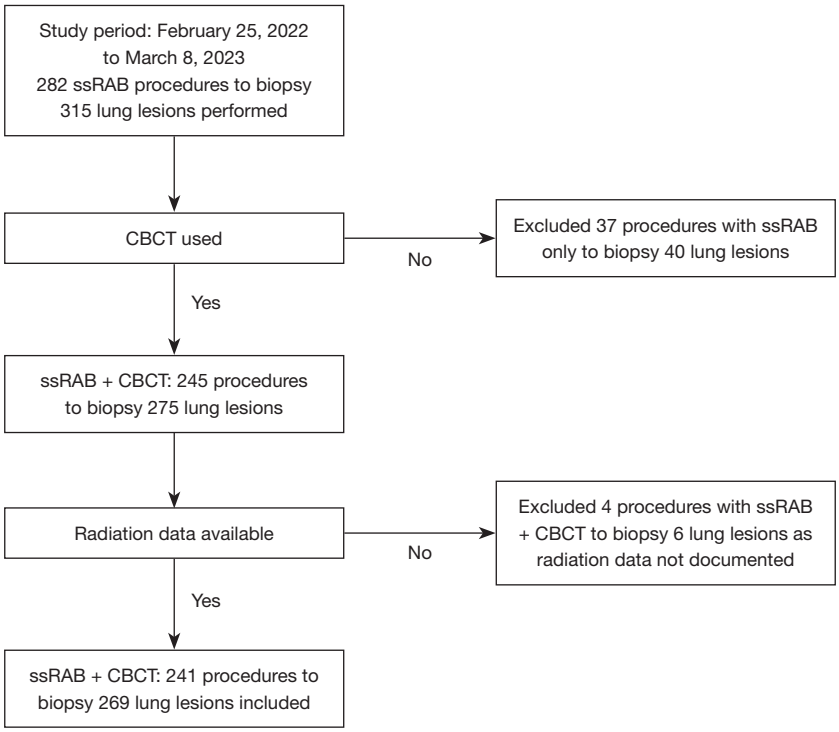

Figure 3 Flowchart with inclusion and exclusion of patients. ssRAB, shape sensing robotic-assisted bronchoscopy; CBCT, cone beam computed tomography.

of nodules were centrally located, with 44.2% in the middle portion of lung and 48.7% located peripherally. There was a right lung predominance at 56.9%, with more nodules located in the upper lobes (33.8% in right upper and 24.2% in left upper). Most of the nodules were solid in appearance (85.1%). *Table 1* summarizes the patient and nodule characteristics.

Procedure characteristics

The total mean bronchoscopy procedure time from the first scope in to the last scope out was 68±28.1 minutes, with the mean RAB portion being 49.2±22.1 minutes. Most procedures only sampled one lesion (89.2%). When multiple lesions were sampled during the procedure, the nodule location was unilateral in 10 cases (38.5%) and bilateral in 16 cases (61.5%). One lesion was not assessed via r-EBUS given concern for bleeding; otherwise, the bronchoscopist utilized r-EBUS to obtain a concentric view in 141 lesions (52.6%), eccentric view in 99 lesions (36.9%), and were unable to visualize the lesion in 28 lesions (10.4%). These numbers represent optimal imaging obtained during the procedure and documented by the bronchoscopist. Mediastinal assessment for staging using linear EBUS, if indicated per bronchoscopist, was performed in 63.1% procedures with mediastinal lymph node or lesion sampling in 41.5% procedures. There was a low rate of complications with eight cases of pneumothoraces (3.3%) with five (2.1%) requiring chest tube placement. No significant bleeding requiring specific additional interventions was observed. *Table 2* summarizes the procedural characteristics.

CBCT characteristics

A mean of 1.5±0.7 (median: 1, range: 1–4) CBCT spins were performed during these procedures. One CBCT spin was performed in 148 procedures (61.4%). The mean total FT was 5.6±2.9 minutes. Sixty-five lesions (24.2%) were visible on conventional fluoroscopy. Mean radiation dose of CAK was 63.5±46.7 mGy and mean DAP was 22.6±16.0 Gy·cm^2. *Table 3* summarizes CBCT and fluoroscopic characteristics. Based on subjective interpretation by the bronchoscopist, as derived from the procedure note, 37 (15.4%) procedures had significant CT-to-body divergence that affected the procedure. Further comparison of patients with or without

Table 1 Patient demographics and nodule characteristics

Variables	Values
Patient demographics (n=241)	
Age (years)	67.8±10.7
Sex	
Female	135 (56.0)
Male	106 (44.0)
BMI (kg/m^2)	27.1±6.5
Current or former tobacco smoker	154 (63.9)
Nodule characteristics (n=269)	
Lesion size dimensions (mm)	
Anteroposterior	18.0±8.8
Transverse	17.2±10.5
Craniocaudal	17.7±10.2
Location	
Central	19 (7.1)
Middle	119 (44.2)
Peripheral	131 (48.7)
Lobe	
Right upper	91 (33.8)
Right middle	19 (7.1)
Right lower	43 (16.0)
Left upper	65 (24.2)
Left lower	51 (19.0)
Lesion characteristic	
Solid	229 (85.1)
Ground glass opacity	13 (4.8)
Mixed	27 (10.0)
Bronchus sign	
Present	158 (58.7)
Absent	111 (41.3)
Spiculation	103 (38.3)
Utilization of radial endobronchial ultrasound to assess nodule	268 (99.6)
Concentric view	141 (52.6)
Eccentric view	99 (36.9)
Unable to confirm	28 (10.4)

Data are presented as mean ± standard deviation or n (%). BMI, body mass index.

Table 2 Procedure characteristics

Characteristics	Values
Total bronchoscopy procedure time (min)	68±28.1
Robotic-assisted bronchoscopy procedure time (min)	49.2±22.1
Nodules biopsied during procedure	
One	215 (89.2)
Two	24 (10.0)
Three	2 (0.8)
Laterality of multiple nodules sampled	
Unilateral	10 (38.5)
Bilateral	16 (61.5)
Mediastinal assessment	152 (63.1)
Mediastinal sampling performed	100 (41.5)
Complications	
Pneumothorax	8 (3.3)
Pneumothorax requiring chest tube	5 (2.1)

Data are presented as mean ± standard deviation or n (%).

significant CT to body divergence was performed (*Table 4*). Significant differences were noted in age, body mass index (BMI), and radiation doses between the groups. Lesion size dimensions were not significantly different between groups.

Diagnostic yield

At index bronchoscopy, 130 lesions (48.3%) had a malignant diagnosis with 101 lesions (37.5%) with a specific benign or non-specific benign diagnosis, with a calculated diagnostic yield of 85.9%. Predictors of diagnostic yield included positive bronchus sign with odds ratio (OR) 2.19 [95% confidence interval (CI): 1.09–4.4; P=0.03], and lesion confirmation with r-EBUS with OR 4.21 (95% CI: 1.77–10.02; P=0.001). The diagnostic yield was 89.9% for lesions with positive and 80.2% with negative bronchus sign, 88.3% with visualization and 64.2% when unable to visualize lesion on r-EBUS.

Among malignant diagnoses, 96 lesions (73.8%) were lung cancer, 27 (20.8%) were metastatic disease, 6 (4.6%) represented malignancy unable to be further identified, and 1 (0.8%) plasma cell neoplasm. Benign diagnosis included:

Table 3 Cone beam CT and fluoroscopy characteristics

Characteristics	Values
Cone beam CT spins performed	1.5±0.7/1 [1–4]
One	148 (61.4)
Two	70 (29.0)
Three	19 (7.9)
Four	4 (1.7)
Significant CT-to-body divergence affecting the procedure	
Yes	37 (15.4)
No	204 (84.6)
Total fluoroscopy time (min)	5.6±2.9
Target visible with fluoroscopy	
Yes	65 (24.2)
No	204 (75.8)
Radiation dose	
Cumulative air kerma (mGy)	63.5±46.7
Cumulative DAP (Gy·cm^2)	22.6±16.0

Data are presented as mean ± standard deviation or median [range] or n (%). CT, computed tomography; DAP, dose area product.

acute or chronic inflammation (n=27, 26.7%), granuloma without identified infection (n=23, 22.8%), organizing pneumonia (n=15, 14.9%), mycobacterial infection (n=10, 9.9%), fungal infection (n=5, 5.0%), bacterial infection (n=2, 2.0%), fibrosis/apical cap (n=6, 5.9%), interstitial lung disease (n=6, 5.9%), lymphoid population (n=2, 2.0%), post radiation changes (n=1, 1.0%), pulmonary infarct (n=1, 1.0%), pleomorphic adenoma (n=1, 1.0%), silicotic nodule (n=1, 1.0%), lipoid pneumonia (n=1, 1.0%).

Discussion

This prospective observational study describes several key radiographic characteristics related to the use of ssRAB combined with CBCT in the evaluation of pulmonary lesions. Evaluating 241 ssRAB procedures to sample 269 lung lesions at our institution revealed the mean total FT was 5.6±2.9 minutes with mean cumulative DAP 22.6±16.0 Gy·cm^2. We describe the use of intraprocedural support from an RT(R), which optimized settings, safety and utilization of radiologic equipment during the procedure. No prior mention of a dedicated radiologic operator for CBCT in conjunction with bronchoscopy has been reported to our knowledge. Most studies do not

Table 4 Comparison of factors between procedures with no or significant CT to body divergence reported

Variables	No significant CT to body divergence (n=204)	Significant CT to body divergence (n=37)	P value
Age (years)	68.4±10.5	64.0±11.2	0.02
BMI (kg/m^2)	26.7±5.7	30.5±8.0	<0.001
Cone beam CT spins performed	1.4±0.6	2.1±0.9	<0.001
One	138	10	–
Two	53	17	–
Three	11	8	–
Four	2	2	–
Total fluoroscopy time (min)	5.6±3.0	5.9±2.6	0.530
Radiation dose			
Cumulative air kerma (mGy)	56.9±40.6	99.7±60.4	<0.001
Cumulative DAP (Gy·cm^2)	20.4±15.0	34.6±16.8	<0.001

Data are presented as mean ± standard deviation or n. CT, computed tomography; BMI, body mass index; DAP, dose area product.

comment on the operator of the fluoroscopic or CBCT equipment; Salahuddin *et al.* reported that physicians operated the mobile CBCT C-arm themselves during the procedure (25).

We chose to report the metrics for CBCT radiation dose in CAK and DAP (16,26). These metrics are reported by the CBCT system after acquisition. CAK is defined as the energy extracted from an X-ray beam per unit mass of air in a small, irradiated air volume (Gy). DAP is defined as the product of the dose and beam area (Gy·cm^2), which is measured using an ionization chamber placed between the X-ray tube setup and the patient (27,28). As a basis of comparison for radiation doses, a standard chest CT uses DAP 40–60 Gy·cm^2, and a chest radiograph in posteroanterior (PA) and lateral views uses 0.1–0.3 and 0.3–0.9 Gy·cm^2, respectively (27). There is a range of conversion factors to determine estimates in effective dose in mSv, but it is system specific and dependent on anatomical location (29). As a result, it is difficult to make dose comparisons between different systems and within the literature. We can calculate a mean estimated effective dose of 3.6 mSv per procedure using a conversion factor of 0.16 mSv/Gy·cm^2 (18).

Our data are comparable to the currently published data regarding radiation dose during bronchoscopic biopsy procedures combined with CBCT to sample pulmonary lesions (16,18,25,30-32). Our radiation use may be lower since we did not require a spin for tool in lesion confirmation and utilized lower dose settings on the system as able. Pritchett *et al.* reported 75 patients who underwent biopsy with CBCT guided ENB to sample 93 suspicious lung nodules; the radiation dose in a representative subset of 9 patients was total DAP per case 31±16 Gy·cm^2 with an average of 1.5 CBCT per procedure (18). DiBardino *et al.* reported that 116 patients who underwent CBCT combined with r-EBUS and ultrathin bronchoscopy had a radiation dose of DAP 76.025 Gy·cm^2 (17). Verhoeven *et al.* described their experience of 238 patients undergoing CBCT guided bronchoscopy in which they undertook efforts at radiation dose reduction during procedures over time from DAP 47.5 (effective dose: 14.3 mSv) to 25.4 Gy·cm^2 (effective dose: 5.8 mSv) (30). Reisenauer *et al.* conducted a single-center prospective pilot study of 30 pulmonary lesions using a combination of mobile 3D imaging with CIOS 3D Spin Mobile (Siemens Healthineers, Malvern, PA, USA) and ssRAB. They reported a mean number of spins of 2.5 and DAP of 50.30±32.0 Gy·cm^2 (15). Salahuddin *et al.* reported 51 patients who underwent ultrathin bronchoscopy with r-EBUS and mobile CBCT use with a median FT of 11.2 minutes, median number of CBCT spins of 1 (range, 1–5), and mean DAP from total exposure of 41.92 Gy·cm^2 (25). Here we report radiation use during the use of ssRAB with fixed CBCT in the largest cohort to date. *Table 5* summarizes studies utilizing CBCT combined with navigational bronchoscopy systems for the evaluation of pulmonary lesions that reported radiation data and highlights the variability in reporting (2,15,18,20,25,33-36). We report a comparable diagnostic yield (85.9%) and pneumothorax rate (3.3%) in our cohort.

Comparison to percutaneous lung biopsy procedures is challenging given different advanced imaging modalities are used for guidance including conventional CT (CCT), CT fluoroscopy (CTF) and CBCT, with differences in reported radiation dose that require conversion to effective dose. A retrospective analysis of CBCT guided percutaneous transthoracic lung nodule needle biopsies in 1,108 patients reported the radiation dose was DAP 32.88 Gy·cm^2 with a mean estimated effective radiation dose of 7.3±4.1 mSv (37). A single center retrospective study comparing 35 CBCT to 69 CCT guided lung biopsies showed similar radiation doses (mean effective doses of 3.4±2.1 *vs.* 3.9±0.79 mSv) with comparable outcomes (38). Yang *et al.* reported a decreased effective radiation dose when performing CBCT virtual navigation guided lung biopsy (7.6 mSv) as compared to CCT guided lung biopsy (13.4 mSv) in a cohort of 217 consecutive patients (39). CTF as compared to CCT had similar radiation doses in a meta-analysis including nine studies with 6,998 patients (40). Based on the limited available data, there is suggestion that radiation use in CBCT guided bronchoscopic lung biopsies is comparable to percutaneous modalities.

Our study has several limitations. This single-center, prospective observational study was conducted in an academic center with multiple bronchoscopists with no standardized procedural protocol. Generalizability may be limited given availability and type of CBCT available to bronchoscopists. We had availability of CBCT with a dedicated RT(R) for every ssRAB procedure in our dedicated interventional pulmonary room. During this study period, we performed 282 ssRAB procedures with ~89% utilizing CBCT. It has become routine and standard of care for our patients to utilize these combined technologies.

CBCT radiation data was not routinely stored in the electronic medical record at our institution during the study period, and was manually collected immediately

Table 5 Studies reporting radiation data in CBCT combined with navigational bronchoscopy systems

Study	Navigational bronchoscopy system	No. of lesions	Diagnostic yield	Pneumothorax rate	Fluoroscopy time	Spins performed	Radiation	CBCT system
Benn 2021 (2)	ssRAB	52	86%	3.8%	NR	"All patients with one nodule biopsied underwent 2–3 spins… 7 patients undergoing biopsy of two different nodules underwent 4 CBCT spins"	Mean radiation exposure 1.69±0.56 mGy; mean DLP 750±526 mGycm	Ceiling mounted CBCT with Dyna CT (Siemens)
Bondue 2023 (ENB in CBCT suite arm) (33)	ENB	25	87%	4.0%	NR	Median 3 (range, 1–8)	Cumulative mean radiation exposure 5.6±2.6 mSv (range, 1.7–10.9 mSv)	Allura Clarity FD20 (Philips)
Bowling 2017 (34)	ENB	14	71%	7.1%	Mean 17 min (range, 2–44 min)	NR	Mean radiation exposure 4.3 mSv (range, 3–5 mSv)	Artis Zeego (Siemens)
Katsis 2021 (35)	ENB	29	72.4%	0	Mean 8.8±5.3 min	NR	Mean radiation dose per nodule 259.6±208.2 mGy	Allura Clarity FD20 (Philips)
Podder 2022 (36)	ENB	17	76.0%	0	NR	Mean 3.5±1.5	Mean dose 858.5±553 mGy	Artis Q bi-plane CBCT (Siemens)
Pritchett 2018* (18)	ENB	93	83.7%	4%	Mean 6.2±2.6 min	Mean 1.5	Estimated effective dose related to fluoroscopy 1.5±0.7 mSv and exposure 3.0±1.4 mSv; total DAP 31±16 Gy·cm^2; mean effective dose of 2.0 mSv per CBCT run	Allura Clarity FD20 (Philips)
Reisenauer 2022 (15)	ssRAB	30	93.3%	0	Mean 8.7 min (range, 2–27 min)	Mean 2.5±1.6	Mean DAP 50.30±32.0 Gy·cm^2	Cios-Spin Mobile 3D C-Arm (Siemens)
Salahuddin 2023 (25)	ssRAB	51	78.4%	2.0%	Median 11.2 min (range, 2.9–42.1 min)	Median 1 (range, 1–5); mean 1.82±1.01	Mean DAP from total exposure 41.92±11.35 Gy·cm^2	Cios-Spin Mobile 3D C-Arm (Siemens)
Verhoeven 2021 (ENB and CBCT arm) (20)	ENB	40	75%	3.4%	Mean 7.3 min (range, 2–23 min)	Mean 1.5 (range, 0–3)	NR	Artis Zeego (Siemens)

*, radiation data reported in representative subset of 9 patients. CBCT, cone beam computed tomography; ssRAB, shape sensing robotic assisted bronchoscopy; NR, not reported; DLP, dose length product; CT, computed tomography; ENB, electromagnetic navigational bronchoscopy; DAP, dose area product.

after the procedure. We did not record specific CBCT or fluoroscopy settings for individual procedures. After review of the data for this manuscript, we have since standardized the dose exposure report to be uploaded to the electronic medical record. CBCT usage varied in terms of timing during procedure, but the first spin was typically performed immediately after navigation, with subsequent spins after additional catheter adjustment or to provide tool in lesion confirmation if rapid onsite evaluation (ROSE) was non-diagnostic. The bronchoscopist's preference determined if r-EBUS probe or tools were extended during the CBCT spin. Determination if a patient had significant CT to body divergence that affected the procedure was subjective and reported by the bronchoscopist in their note with no additional calculations made in comparison between pre-procedure and intra-procedural imaging. Although subjective in this study, the determination of significant CT to body divergence as compared to no significant divergence was notable for higher patient BMI and radiation doses (CAK and DAP). We feel that further procedural standardization is possible at this point and can be incorporated in future prospective data collection.

In addition, our patients may have higher total radiation doses overall if we were to also include the radiation from the pre-procedure CT scan; a procedural aspect that was also not commented on by other studies to our knowledge. Due to limited follow-up post bronchoscopy, we only include biopsy results at time of index bronchoscopy; diagnostic yield may change with further follow-up and depending on calculation method used. We report a diagnostic yield of 85.9% and pneumothorax rate of 3.3% in our cohort. It is noteworthy that this yield was obtained based on the recently published methodology for diagnostic yield from bronchoscopic sampling by Vachani *et al.* at the time of index bronchoscopy (24). This is compared to the conventional diagnostic test accuracy methodology used in our recent manuscript with a higher overall yield of 91.4% with a negative predictive value of 81.3% and a sensitivity of 87.3% (4).

Given the current integration of mobile 3D imaging (CIOS 3D Spin Mobile) with ssRAB (41), bronchoscopists will likely use advanced radiologic imaging modalities for diagnostics and future therapeutics. In addition to the goal of improved diagnostic accuracy, other potential benefits with the use of CBCT combined with guided bronchoscopy include reduced procedure or FT if it is easier to visualize the catheter-to-lesion positioning and adjust as compared to other methods.

Compared with other procedural specialties, CBCT is a technology for which bronchoscopists may have had limited training or experience, with a potential additional learning curve in adoption. The literature on advanced diagnostic pulmonary procedures is less robust regarding acceptable or standardized radiation use and best practices compared to other specialties (42,43). Radiation exposure or dose has not been routinely reported in the advanced diagnostic bronchoscopy literature. As an example, the large multi-center NAVIGATE trial only reported if fluoroscopy or CBCT was used during the procedure without additional specifics (44-46).

In terms of safety, the United States Nuclear Regulatory Commission has established an annual occupational total effective dose equivalent for the whole body of 5,000 mrem (50 mSv) and requires all individuals who are likely to receive a dose of more than 100 mrem (1 mSv) to receive adequate training (47). For comparison, the "average" American receives about 620 mrem (6.2 mSv) per year from all sources of radiation and a full body CT scan is 1,000 mrem (10 mSv) (48). All staff at our institution who work in areas with fluoroscopy or radiation are required to undergo yearly training and wear radiation dosimeters to monitor exposure. As these dosimeters are worn by the bronchoscopists and staff for all procedures with ionizing radiation, they represent doses for all pulmonary procedures, not just ssRAB with CBCT, and this data is not included. Bronchoscopists should be cognizant of radiation use during the procedure and have a goal for "as low as reasonably achievable" (ALARA) doses for both patient and staff safety (28). Practices for ALARA include setting CBCT and fluoroscopy to the lowest dose settings possible, utilizing pulsed fluoroscopy when possible, and only performing the minimum necessary runs of CBCT or fluoroscopy to successfully and safely complete the procedure.

Conclusions

This prospective study adds to the current body of literature describing radiation dose with the use of a specific system fixed CBCT combined with ssRAB for biopsy of pulmonary lesions. Additional prospective data, systems-specific information and comparable studies are necessary to establish a standardized acceptable radiation dose for bronchoscopic procedures, with coordinated efforts to reduce radiation exposure for patients and staff. Our study

also raises questions regarding the potential role of a dedicated registered radiologic technologist, RT(R) during bronchoscopic procedures.

Acknowledgments

The authors wish to thank the hybrid operating room radiologic technologists at UT Southwestern for their assistance in performing these procedures.
Funding: None.

Footnote

Reporting Checklist: The authors have completed the STROBE reporting checklist. Available at https://jtd.amegroups.com/article/view/10.21037/jtd-23-587/rc

Data Sharing Statement: Available at https://jtd.amegroups.com/article/view/10.21037/jtd-23-587/dss

Peer Review File: Available at https://jtd.amegroups.com/article/view/10.21037/jtd-23-587/prf

Conflicts of Interest: All authors have completed the ICMJE uniform disclosure form (available at https://jtd.amegroups.com/article/view/10.21037/jtd-23-587/coif). AS is a member of the Ambu advisory board. This role is unrelated to this study. AS is a volunteer member of the AABIP Advocacy Committee. AS and KS have received travel and lodging support to attend educational conferences sponsored by Intuitive Surgical. The other authors have no conflicts of interest to declare.

Ethical Statement: The authors are accountable for all aspects of the work in ensuring that questions related to the accuracy or integrity of any part of the work are appropriately investigated and resolved. The study was conducted in accordance with the Declaration of Helsinki (as revised in 2013). The study was approved by UT Southwestern Institutional Review Board (No. STU-2021-0346) and individual consent for this analysis was waived.

References

1. Fielding DIK, Bashirzadeh F, Son JH, et al. First Human Use of a New Robotic-Assisted Fiber Optic Sensing Navigation System for Small Peripheral Pulmonary Nodules. Respiration 2019;98:142-50.
2. Benn BS, Romero AO, Lum M, et al. Robotic-Assisted Navigation Bronchoscopy as a Paradigm Shift in Peripheral Lung Access. Lung 2021;199:177-86.
3. Kalchiem-Dekel O, Connolly JG, Lin IH, et al. Shape-Sensing Robotic-Assisted Bronchoscopy in the Diagnosis of Pulmonary Parenchymal Lesions. Chest 2022;161:572-82.
4. Styrvoky K, Schwalk A, Pham D, et al. Shape-Sensing Robotic-Assisted Bronchoscopy with Concurrent use of Radial Endobronchial Ultrasound and Cone Beam Computed Tomography in the Evaluation of Pulmonary Lesions. Lung 2022;200:755-61.
5. Oberg CL, Lau RP, Folch EE, et al. Novel Robotic-Assisted Cryobiopsy for Peripheral Pulmonary Lesions. Lung 2022;200:737-45.
6. Pritchett MA, Bhadra K, Calcutt M, et al. Virtual or reality: divergence between preprocedural computed tomography scans and lung anatomy during guided bronchoscopy. J Thorac Dis 2020;12:1595-611. Erratum in: J Thorac Dis 2020;12:4593-5.
7. Chen A, Pastis N, Furukawa B, et al. The effect of respiratory motion on pulmonary nodule location during electromagnetic navigation bronchoscopy. Chest 2015;147:1275-81.
8. Salahuddin M, Sarkiss M, Sagar AS, et al. Ventilatory Strategy to Prevent Atelectasis During Bronchoscopy Under General Anesthesia: A Multicenter Randomized Controlled Trial (Ventilatory Strategy to Prevent Atelectasis -VESPA- Trial). Chest 2022;162:1393-401.
9. Pritchett MA, Lau K, Skibo S, et al. Anesthesia considerations to reduce motion and atelectasis during advanced guided bronchoscopy. BMC Pulm Med 2021;21:240.
10. Ravikumar N, Ho E, Wagh A, et al. Advanced Imaging for Robotic Bronchoscopy: A Review. Diagnostics (Basel) 2023;13:990.

11. Orth RC, Wallace MJ, Kuo MD, et al. C-arm cone-beam CT: general principles and technical considerations for use in interventional radiology. J Vasc Interv Radiol 2008;19:814-20.
12. Ng CSH, Man Chu C, Kwok MWT, et al. Hybrid DynaCT scan-guided localization single-port lobectomy. Chest 2015;147:e76-8. Erratum in: Chest 2015;147:1445.
13. Glatz AC, Zhu X, Gillespie MJ, et al. Use of angiographic CT imaging in the cardiac catheterization laboratory for congenital heart disease. JACC Cardiovasc Imaging 2010;3:1149-57.
14. Setser R, Chintalapani G, Bhadra K, et al. Cone beam CT imaging for bronchoscopy: a technical review. J Thorac Dis 2020;12:7416-28.
15. Reisenauer J, Duke JD, Kern R, et al. Combining Shape-Sensing Robotic Bronchoscopy With Mobile Three-Dimensional Imaging to Verify Tool-in-Lesion and Overcome Divergence: A Pilot Study. Mayo Clin Proc Innov Qual Outcomes 2022;6:177-85.
16. Casal RF, Sarkiss M, Jones AK, et al. Cone beam computed tomography-guided thin/ultrathin bronchoscopy for diagnosis of peripheral lung nodules: a prospective pilot study. J Thorac Dis 2018;10:6950-9.
17. DiBardino DM, Kim RY, Cao Y, et al. Diagnostic Yield of Cone-beam-Derived Augmented Fluoroscopy and Ultrathin Bronchoscopy Versus Conventional Navigational Bronchoscopy Techniques. J Bronchology Interv Pulmonol 2022. [Epub ahead of print]. doi: 10.1097/LBR.0000000000000883.
18. Pritchett MA, Schampaert S, de Groot JAH, et al. Cone-Beam CT With Augmented Fluoroscopy Combined With Electromagnetic Navigation Bronchoscopy for Biopsy of Pulmonary Nodules. J Bronchology Interv Pulmonol 2018;25:274-82.
19. Kheir F, Thakore SR, Uribe Becerra JP, et al. Cone-Beam Computed Tomography-Guided Electromagnetic Navigation for Peripheral Lung Nodules. Respiration 2021;100:44-51.
20. Verhoeven RLJ, Fütterer JJ, Hoefsloot W, et al. Cone-Beam CT Image Guidance With and Without Electromagnetic Navigation Bronchoscopy for Biopsy of Peripheral Pulmonary Lesions. J Bronchology Interv Pulmonol 2021;28:60-9.
21. Casal RF, Sepesi B, Sagar AS, et al. Centrally located lung cancer and risk of occult nodal disease: an objective evaluation of multiple definitions of tumour centrality with dedicated imaging software. Eur Respir J 2019;53:1802220.
22. Harris PA, Taylor R, Thielke R, et al. Research electronic data capture (REDCap)--a metadata-driven methodology and workflow process for providing translational research informatics support. J Biomed Inform 2009;42:377-81.
23. Harris PA, Taylor R, Minor BL, et al. The REDCap consortium: Building an international community of software platform partners. J Biomed Inform 2019;95:103208.
24. Vachani A, Maldonado F, Laxmanan B, et al. The Effect of Definitions and Cancer Prevalence on Diagnostic Yield Estimates of Bronchoscopy: A Simulation-Based Analysis. Ann Am Thorac Soc 2023. [Epub ahead of print]. doi: 10.1513/AnnalsATS.202302-182OC.
25. Salahuddin M, Bashour SI, Khan A, et al. Mobile Cone-Beam CT-Assisted Bronchoscopy for Peripheral Lung Lesions. Diagnostics (Basel) 2023;13:827.
26. Sciahbasi A, Frigoli E, Sarandrea A, et al. Radiation Exposure and Vascular Access in Acute Coronary Syndromes: The RAD-Matrix Trial. J Am Coll Cardiol 2017;69:2530-7.
27. Nickoloff EL, Lu ZF, Dutta AK, et al. Radiation dose descriptors: BERT, COD, DAP, and other strange creatures. Radiographics 2008;28:1439-50.
28. Stecker MS, Balter S, Towbin RB, et al. Guidelines for patient radiation dose management. J Vasc Interv Radiol 2009;20:S263-73.
29. Hohenforst-Schmidt W, Banckwitz R, Zarogoulidis P, et al. Radiation Exposure of Patients by Cone Beam CT during Endobronchial Navigation - A Phantom Study. J Cancer 2014;5:192-202.
30. Verhoeven RLJ, van der Sterren W, Kong W, et al. Cone-beam CT and Augmented Fluoroscopy-guided Navigation Bronchoscopy: Radiation Exposure and Diagnostic Accuracy Learning Curves. J Bronchology Interv Pulmonol 2021;28:262-71.
31. Avasarala SK, Machuzak MS, Gildea TR. Multidimensional Precision: Hybrid Mobile 2D/3D C-Arm Assisted Biopsy of Peripheral Lung Nodules. J Bronchology Interv Pulmonol 2020;27:153-5.
32. Yu KL, Yang SM, Ko HJ, et al. Efficacy and Safety of Cone-Beam Computed Tomography-Derived Augmented Fluoroscopy Combined with Endobronchial Ultrasound in Peripheral Pulmonary Lesions. Respiration 2021;100:538-46.
33. Bondue B, Taton O, Tannouri F, et al. High diagnostic yield of electromagnetic navigation bronchoscopy performed under cone beam CT guidance: results of a randomized Belgian monocentric study. BMC Pulm Med 2023;23:185.

34. Bowling MR, Brown C, Anciano CJ. Feasibility and Safety of the Transbronchial Access Tool for Peripheral Pulmonary Nodule and Mass. Ann Thorac Surg 2017;104:443-9.
35. Katsis J, Roller L, Lester M, et al. High Accuracy of Digital Tomosynthesis-Guided Bronchoscopic Biopsy Confirmed by Intraprocedural Computed Tomography. Respiration 2021. [Epub ahead of print]. doi: 10.1159/000512802.
36. Podder S, Chaudry S, Singh H, et al. Efficacy and Safety of Cone-Beam CT Augmented Electromagnetic Navigation Guided Bronchoscopic Biopsies of Indeterminate Pulmonary Nodules. Tomography 2022;8:2049-58.
37. Lee SM, Park CM, Lee KH, et al. C-arm cone-beam CT-guided percutaneous transthoracic needle biopsy of lung nodules: clinical experience in 1108 patients. Radiology 2014;271:291-300.
38. Cheng YC, Tsai SH, Cheng Y, et al. Percutaneous Transthoracic Lung Biopsy: Comparison Between C-Arm Cone-Beam CT and Conventional CT Guidance. Transl Oncol 2015;8:258-64.
39. Yang L, Wang Y, Li L, et al. C-Arm Cone-Beam CT Virtual Navigation versus Conventional CT Guidance in the Transthoracic Lung Biopsy: A Case-Control Study. Diagnostics (Basel) 2022;12:115.
40. Fu YF, Li GC, Cao W, et al. Computed Tomography Fluoroscopy-Guided Versus Conventional Computed Tomography-Guided Lung Biopsy: A Systematic Review and Meta-analysis. J Comput Assist Tomogr 2020;44:571-7.
41. Intuitive and Siemens Healthineers enhance scanning integration for Ion Endoluminal procedures. Available online: https://isrg.intuitive.com/news-releases/news-release-details/intuitive-and-siemens-healthineers-enhance-scanning-integration
42. Hirshfeld JW Jr, Ferrari VA, Bengel FM, et al. 2018 ACC/HRS/NASCI/SCAI/SCCT Expert Consensus Document on Optimal Use of Ionizing Radiation in Cardiovascular Imaging: Best Practices for Safety and Effectiveness: A Report of the American College of Cardiology Task Force on Expert Consensus Decision Pathways. J Am Coll Cardiol 2018;71:e283-351.
43. Miller DL, Vañó E, Bartal G, et al. Occupational radiation protection in interventional radiology: a joint guideline of the Cardiovascular and Interventional Radiology Society of Europe and the Society of Interventional Radiology. Cardiovasc Intervent Radiol 2010;33:230-9.
44. Khandhar SJ, Bowling MR, Flandes J, et al. Electromagnetic navigation bronchoscopy to access lung lesions in 1,000 subjects: first results of the prospective, multicenter NAVIGATE study. BMC Pulm Med 2017;17:59.
45. Folch EE, Pritchett MA, Nead MA, et al. Electromagnetic Navigation Bronchoscopy for Peripheral Pulmonary Lesions: One-Year Results of the Prospective, Multicenter NAVIGATE Study. J Thorac Oncol 2019;14:445-58.
46. Folch EE, Bowling MR, Pritchett MA, et al. NAVIGATE 24-Month Results: Electromagnetic Navigation Bronchoscopy for Pulmonary Lesions at 37 Centers in Europe and the United States. J Thorac Oncol 2022;17:519-31.
47. Information for Radiation Workers. Available online: https://www.nrc.gov/about-nrc/radiation/health-effects/info.html
48. Radiation All Around Us. Available online: https://www.nrc.gov/about-nrc/radiation/around-us/doses-daily-lives.html

Cite this article as: Styrvoky K, Schwalk A, Pham D, Madsen K, Chiu HT, Abu-Hijleh M. Radiation dose of cone beam CT combined with shape sensing robotic assisted bronchoscopy for the evaluation of pulmonary lesions: an observational single center study. J Thorac Dis 2023;15(9):4836-4848. doi: 10.21037/jtd-23-587